Demonstration of 0.75 Gbar Planar Shocks in X-Ray Driven Colliding Foils

R. Cauble, D. W. Phillion, T. J. Hoover,[a] N. C. Holmes, J. D. Kilkenny, and R. W. Lee
Lawrence Livermore National Laboratory, University of California, Livermore, California 94550
(Received 30 November 1992)

We have directly observed 0.75 ± 0.2 Gbar planar shocks in gold target foils impacted by ablatively driven gold flyer foils. The x-ray drive for the flyer foils was produced in a gold *Hohlraum* by ten beams of the Nova laser. The dynamic pressure inferred by shock velocity measurements is more than a factor of 7 greater than previous dynamic shocks produced in the laboratory and over a surface area significantly larger than most previous ultrahigh pressure experiments. The technique allows the laboratory investigation of equations of state in the gigabar regime.

PACS numbers: 62.50.+p, 07.35.+k, 64.30.+t

Material pressures of hundreds of millions of atmospheres (hundreds of megabars—Mbar) are common in astrophysical objects and are predicted to exist in the laboratory in spherically compressed capsules typical of inertial confinement fusion targets [1]. Knowledge of the equation of state (EOS) for this regime is thus important to describe the thermodynamics and hydrodynamics of these systems. In the limiting case of extremely high pressure, the EOS can be described by a Thomas-Fermi model; however, the regime of applicability and approach to this limit are not known [2]. Until now, this regime has been unexplored in the laboratory because of the necessity to produce conditions approaching one gigabar (Gbar) in a geometry which allows the state of the system to be measured, viz., planar geometry. We have produced the first direct measurement of shock velocities indicative of pressures in this regime in the laboratory. The pressures we determine are in excess of 0.7 Gbar. This was accomplished in planar geometry using a flyer foil driven by x rays from a cavity illuminated by beams of the Nova laser.

EOS data in the 1–2 Mbar regime can be measured in the laboratory by diamond anvil techniques [3]. Higher pressures can be achieved through the use of dynamic shocks, the measurements of which can lead to models for the EOS [4]. For planar shocks, direct irradiation of solids with a single high intensity laser extended this regime up to about 30 Mbar [5]; laser driven impedance mismatch experiments have allowed laboratory experiments to reach pressures from 30 Mbar to greater than 50 Mbar [6]. Overlapping two high intensity beams has led to inferred pressures of nearly 100 Mbar [7]. These latter data indicate that material conditions can be reached in the laboratory which are comparable with conditions in nuclear weapon driven EOS experiments, which have provided valuable data for equations of state in the sub-100-Mbar regime [8]. Experience with laser driven foils suggested that these foils could be used to impact stationary disks in order to reach even higher pressures [9]. In this method, the flyer stores kinetic energy from the driver over an acceleration time and delivers it much more rapidly as thermal energy in collision. In addition, the flyer acts as a preheat shield so that the target remains on a lower adiabat than if it were exposed to the driver. These attributes make it possible to achieve much higher pressures using a flyer-impact configuration than with a directly driven configuration [10]. This technique was successfully demonstrated using a laser as a driver [11] and later applied to achieve pressures of more than 100 Mbar [12].

Several problems must be overcome when using this technique. First, in all cases where a laser is utilized as a driving source, the laser must be spatially uniform. If not, resulting uneven deposition leads to hot spots and consequent generation of high energy electrons, penetrating radiation, and hydrodynamic instability of the irradiated foil. Second, penetrating radiation, which can preheat the target foil, can also be produced in laser-plasma interactions by the very high intensity which is required to drive the foil to the high velocities necessary to reach 100 Mbar pressures in collision [12]. Third, the required high driver intensities mean that focal spot sizes must be small (≈ 50 μm) for low energy lasers, so that the experiment becomes manifestly two dimensional: Shock decay and matter motion perpendicular to the beam become significant [12,13]. When such nonplanarity of the shock occurs, the measurements must be interpreted through two-dimensional simulation. Last, a directly irradiated foil is prone to Rayleigh-Taylor instability necessitating a small acceleration distance between flyer and target foils; this problem can be ameliorated by use of an ablator [14]. To circumvent these problems and move on to a new regime of investigation, we have performed a set of experiments which utilize a high intensity x-ray drive which is uniform over a large area, more than 500 μm. This drive accelerates a foil which then collides with a preheat-free stationary foil producing a pressure of over 700 Mbar in a planar shock. Because of the large size of the experimental target assembly and the drive uniformity, the results do not require two-dimensional interpretation and our results are simulation independent.

The experimental arrangement is illustrated in Fig. 1. The drive was created by focusing Nova's ten beams (a total of 25 kJ of 0.35 μm light in 1 nsec) into a gold

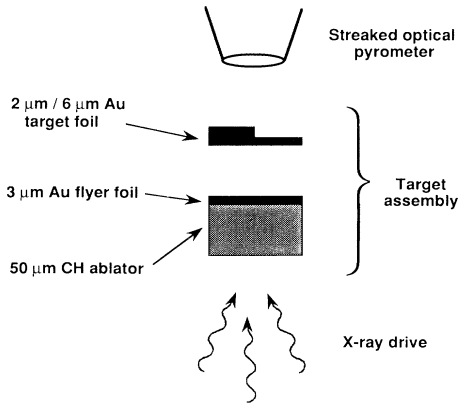

FIG. 1. Overview of the experimental arrangement. The diagram is not to scale. The main components are (1) x-ray drive; (2) target assembly composed of the CH ablator, the 3 μm Au flyer foil, a 50 μm void, and the two-thickness Au target foil, all held in an unshown sleeve; and (3) streaked optical pyrometer.

Hohlraum, converting a significant fraction of laser light to x rays. The x rays ablate a 50 μm layer of polystyrene to which is attached a 3 μm thick gold foil. This flyer foil accelerates through a 50 μm void region and collides with a stationary gold target foil made of two thicknesses, 2 and 6 μm, launching a compression wave into both foils. When the shock breaks out on the back side of the target foil, the high temperature material is imaged through a 60 μm slit onto a time-calibrated streaked optical pyrometer [15]. The image shows shock breakout at two times corresponding to the two thicknesses; the time interval between the breakouts measures the shock speed in the target, assuming the shock speed is constant. By reference to an equation of state, the properties of the shocked matter, such as pressure, density, and temperature can be inferred from the shock speed. If a second parameter of the shocked material could be measured, the Hugoniot part of the equation of state could be determined.

The cylindrical target assembly was mounted across a hole in the wall of the *Hohlraum* with the ablator facing the *Hohlraum* interior. Target assembly sizes were more than 0.5 mm in diameter. The approximately 100 μm long target assembly was placed at the bottom of a 1 mm gold sleeve so that the assembly was completely shielded from unfocused, unconverted laser light. Additional shielding prevented the diagnostic from viewing heated areas of the sleeve and the *Hohlraum.*

Any slight spatial imbalance in the drive or any unpredicted edge effects, due, e.g., to interactions between the flyer foil and the sleeve, could cause the flyer to tilt or curve, which would drive a nonplanar shock into the target and compromise the interpretation. Because of these considerations, the entire target assembly including the aperture were constructed with a large diameter -500 μm on three experiments and 700 μm on the remaining three experiments—so that any nonplanarity in shock breakout could be observed. The x-ray drive from the *Hohlraum* for two shots performed without a target foil in place was observed to be sufficiently uniform so that a 0.5 mm diameter was acceptable. In addition, the step in the target was at the center of the large foil, where the effects of edge-induced nonuniformities would be minimized. Temporal resolution of the streak camera dictated a minimum difference of 4 μm between the thin and thick parts of the target foil. The thin part of the target foil was chosen to be 2 μm to minimize preheating of the streak-camera-viewed rear side of the target foil. These considerations indicated that a target foil composed of a 2 μm and a 6 μm part be used.

Figure 2(a) shows a streak camera record from a typical experiment, where shock breakout across the two steps is clearly evident. Two spatially averaged densitometer traces converted to exposure are taken along the dashed lines indicated in Fig. 2(a), and are shown in Fig. 2(b). The two traces are signals from the rear side of the target foil on either side of the central step. Examination of the traces indicates an interval of 57 ± 5 ps between breakout on the two thicknesses, corresponding to an average shock velocity of 70 ± 6 km/sec. From the SESAME equation of state tables [16], this shock speed corresponds to a density of 90 g/cm^3 and a pressure of 0.74 Gbar in the gold target.

Table I is a compilation of the results of the six experiments performed. There were no significant differences in drive conditions for all these experiments, except experiment 6, which will be described below. The latter four experiments fall into a group with pressures between 0.64 and 0.83 Gbar. The first two experiments were significantly outside this range. However, the large spatial extent of the streak records clearly showed uneven shock breakout resulting from deformed target foils, likely occurring when the assemblies were pumped down to vacuum. The later experimental assemblies were fabricated in an improved manner allowing for greater strength and precision. Thus we believe that the earlier experiments can be discounted.

The largest single unknown is the target foil preheat. If the target foil suffers any heating before the flyer-target collision, the thinner side will have a higher energy density than the thicker side. In this case, enough mass near the surface of the thinner step could lift off to significantly alter the interpretation of the measurements: Mass ablating off the back side of the target foil effectively makes the 2 μm step thicker, so that the shock on that side breaks out later. The shortened measured interval time would imply an enhanced pressure in the target. Given the mass of material between the drive and the target foil, the only source of target preheat would arise from very high energy x rays. To test this possibility, the x-ray drive was altered in one experiment, that is, number 6 in Table I, so that the overall drive intensity was identical to those in the previous experiments, but the

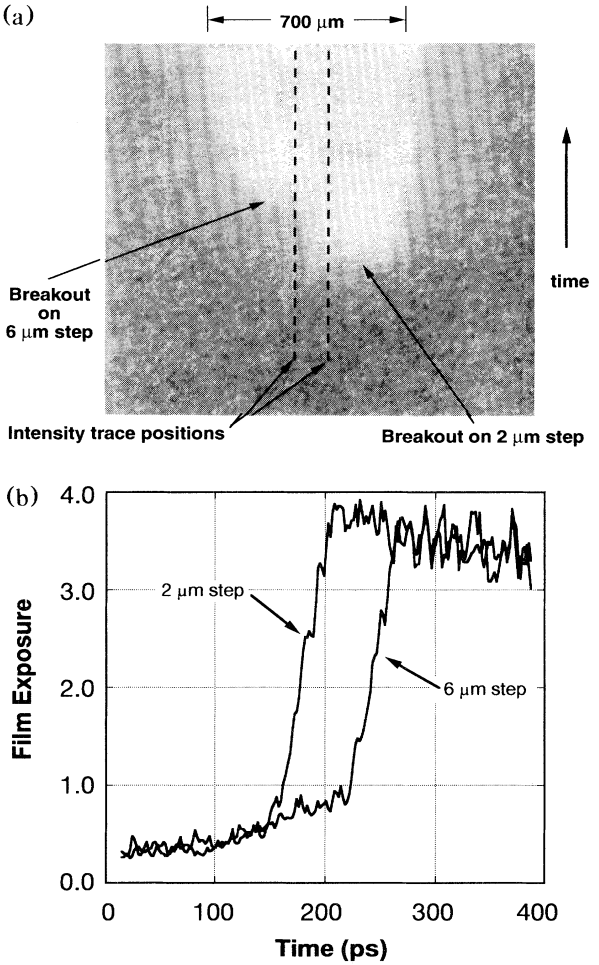

FIG. 2. Data from one experiment. (a) Streak camera record of the rear side of the target foil showing the illumination of shock breakouts on the 2 μm, earlier, and 6 μm, later, sides; (b) intensity traces vs time taken on either side of the step, along the dashed lines shown in (a). The interval between the traces provides the shock travel time across the 4 μm step difference. The interval is about 57 psec, indicating a shock speed of 70 km/sec. From the SESAME EOS tables a pressure of 0.74 Gbar is deduced from this shock speed [16].

intensity of high energy x rays, those ≥ 2.5 keV, was reduced by more than a factor of 5. The result was well within the uncertainties of the three previous nominal experiments; so, we do not believe our results are affected by drive preheat. We have not discussed preheat of the target foil by the shock itself, since this should be identical for both thicknesses; however, evidence of this may be seen in Fig. 2(b) as a small, rising signal prior to breakout. Since the strongly shocked material is expected to reach a temperature of approximately 100 eV [16], this signal is evidently radiation from this hot matter transported through the remaining unshocked gold. This distance ahead of the shock which is heated in this manner is expected to be small, since thermal photon mean free paths in nominal density metals are a few hundred angstroms [17].

TABLE I. Data taken from six experiments. *Interval* is the measured time difference, in picoseconds, between shock breakouts on the two steps at 2 μm and 6 μm as determined from the film record; U_s is the corresponding mean shock speed, in km/sec, over the 4 μm distance between the steps; ρ and P represent values of density, in g/cm^3, and pressure, in gigabars, corresponding to U_s along the principal Hugoniot as predicted by the SESAME equation of state tables [16]. Note that after experiments 1 and 2, the targets were made by an improved method.

Expt.	Interval (psec)	U_s (km/sec)	ρ (g/cm^3)	P (Gbar)
1	86.0 ± 7	47.0 ± 4	80.0 ± 2	0.32 ± 0.05
2	39.0 ± 5	103.0 ± 13	100.0 ± 3	1.60 ± 0.41
3	54.0 ± 7	74.0 ± 9	91.0 ± 2	0.83 ± 0.21
4	62.0 ± 10	65.0 ± 10	88.0 ± 3	0.64 ± 0.20
5	57.0 ± 5	70.0 ± 6	90.0 ± 2	0.74 ± 0.13
6	58.0 ± 7	69.0 ± 8	90.0 ± 2	0.72 ± 0.17

An extension of this technique can be made in order to obtain EOS data in the several hundred Mbar regime. If the flyer foil can be shielded so that the flyer does not significantly heat or decompress, data points on the Hugoniot can be found by measuring the speed of the flyer foil [10]. Since the target foils are observed to stay intact until collision, this can be accomplished by modifying the target foil as shown in Fig. 3. In addition to the shock speed measured as above, the flyer speed can be simultaneously obtained by recording shock breakouts from two identically thick foils placed at different distances along the flyer path. The large diameter and one-dimensional nature of the experiment make this arrangement practicable. To test the feasibility of this technique, we performed one experiment with a three-step Au target foil. Although the condition of the flyer foil was un-

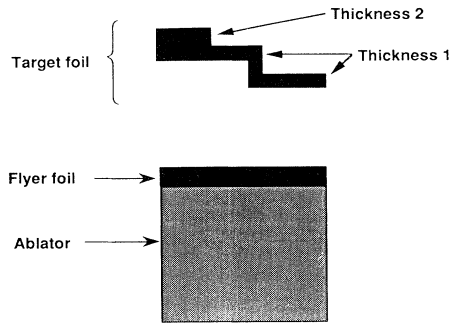

FIG. 3. A target foil configuration which will allow the simultaneous measurement of shock speed and flyer speed. From the latter, the material speed behind the shock can be inferred [10]. These two measurements will allow the calculation of a primary data point on the Hugoniot in the Gbar regime.

known, so that we could not evaluate a Hugoniot data point (nor do we expect the flyer foil to remain intact in the present configuration), we did observe shock breakout from all three steps, indicating the viability of the approach.

Since the data we have determined here are simulation independent we can use them to test the adequacy of our simulation capability. To this end we have studied these experiments with the LASNEX simulation code [18].

First, we examined the experiments as illustrated in Fig. 1. For these cases the simulations indicated that the flyer foil would begin to accelerate about 0.5 nsec after initiation of the laser pulse. The bulk of the flyer was predicted to decompress from its initial density of 19.3 g/cm^3 to approximately 10 g/cm^3. Near the end of the pulse, the flyer was predicted to collide with the target foil producing a shock with a pressure of 0.8–1.0 Gbar throughout most of the thickness of the target, somewhat above what we inferred from the data. Further, simulations indicated that the 6 μm target foil thickness is sufficiently thin so that the shock would not significantly decay in transit. LASNEX indicated that the ≈ 1 Gbar pressure is maintained in the shocked gold for about 30 psec after passage of the shock front, decaying to ≈ 300 Mbar 100 psec after passage. Second, we examined the experimental configuration illustrated in Fig. 3. For this case the measured speed of the flyer generally matched the simulation predictions of tens of km/sec and the pressure inferred during collision was over 0.7 Gbar. While the simulation results are obviously dependent on various code parameters, LASNEX was found to predict the bulk hydrodynamic properties of these experiments.

In conclusion, we have produced the first inferred measurement of pressures of more than 0.7 Gbar in the laboratory. This was accomplished in planar geometry using the flyer foil technique, in which the flyer was driven by x rays from a cavity illuminated by the Nova laser. The target foil was observed to be unaffected by drive preheat and the large size of the foil made small two-dimensional effects observable. We also suggest a method by which this technique may be applied to provide primary data on the equation of state of matter in the gigabar regime.

We would like to acknowledge the assistance of J. D. Johnson and S. Lyon of LANL for supplying the SESAME Hugoniot data. We also note helpful discussions with L. B. DaSilva and J. S. Wark. This work was performed under the auspices of the U.S. Department of Energy by Lawrence Livermore National Laboratory under Contract No. W-7405-ENG-48.

---

[a]Present address: Defense Nuclear Agency, Alexandria, VA 22310.

[1] J. D. Lindl *et al.*, Phys. Today **45**, No. 9, 32 (1992).

[2] A. V. Bushman and V. E. Fortov, Usp. Fiz. Nauk **140**, 177 (1983) [Sov. Phys. Usp. **26**, 465 (1983)].

[3] See, e.g., R. J. Hemley and H. K. Mao, Phys. Rev. Lett. **61**, 857 (1988).

[4] L. V. Al'tshuler, Usp. Fiz. Nauk **85**, 197 (1965) [Sov. Phys. Usp. **8**, 52 (1965)].

[5] L. R. Veeser and S. C. Solem, Phys. Rev. Lett. **40**, 1391 (1978); R. J. Trainor *et al.*, Phys. Rev. Lett. **42**, 1154 (1979); F. Cottet *et al.*, Phys. Rev. Lett. **52**, 1884 (1984).

[6] N. C. Holmes, *et al.*, in *Proceedings of the Eighth AIRAPT and Nineteenth EHPRG Conference,* edited by C. M. Backman, T. Johannisson, and L. Thenér (University of Uppsala, Uppsala, 1981); F. Cottet, Appl. Phys. Lett. **47**, 678 (1985).

[7] J. D. Kilkenny, University of California Report No. UCRL 50021-86, 1987 (unpublished), pp. 3–6.

[8] C. E. Ragan III, Phys. Rev. A **29**, 1391 (1984).

[9] R. J. Harrach and A. Szoke, University of California Report No. UCRL-86798, 1982 (unpublished); R. F. Schmaltz and J. Meyer-ter-Veyn, Phys. Fluids **28**, 932 (1985).

[10] Ya. B. Zel'dovich and Yu. P. Raizer, *Physics of Shock Waves and High-Temperature Hydrodynamic Phenomena* (Academic, New York, 1967), Vol. II, p. 724.

[11] S. P. Obenschain *et al.*, Phys. Rev. Lett. **50**, 44 (1983).

[12] R. Fabbro, B. Faral, J. Virmont, H. Pepin, F. Cottet, and J. P. Romain, Laser Part. Beams **4**, 413 (1986).

[13] B. Faral *et al.*, in *Shock Waves in Condensed Matter 1987,* edited by S. C. Schmidt and N. C. Holmes (Elsevier, Amsterdam, 1988).

[14] S. E. Bodner, Phys. Rev. Lett. **33**, 761 (1974); L. D. Lindl and W. C. Mead, Phys. Rev. Lett. **34**, 1273 (1975).

[15] V. W. Slivinsky and R. P. Drake, University of California Report No. UCRL 50021-84, 1985 (unpublished), pp. 5–90.

[16] "T-4 Handbook of Material Properties Data Bases: Vol. 1c, Equations of State," edited by K. S. Holian, LANL Report No. LA-10160-MS, UC-34, November, 1984 (unpublished).

[17] *Physics of Shock Waves and High Temperature Hydrodynamic Phenomena* (Ref. [10]), p. 771.

[18] G. B. Zimmerman and W. L. Kruer, Comments Plasma Phys. **2**, 51 (1975).

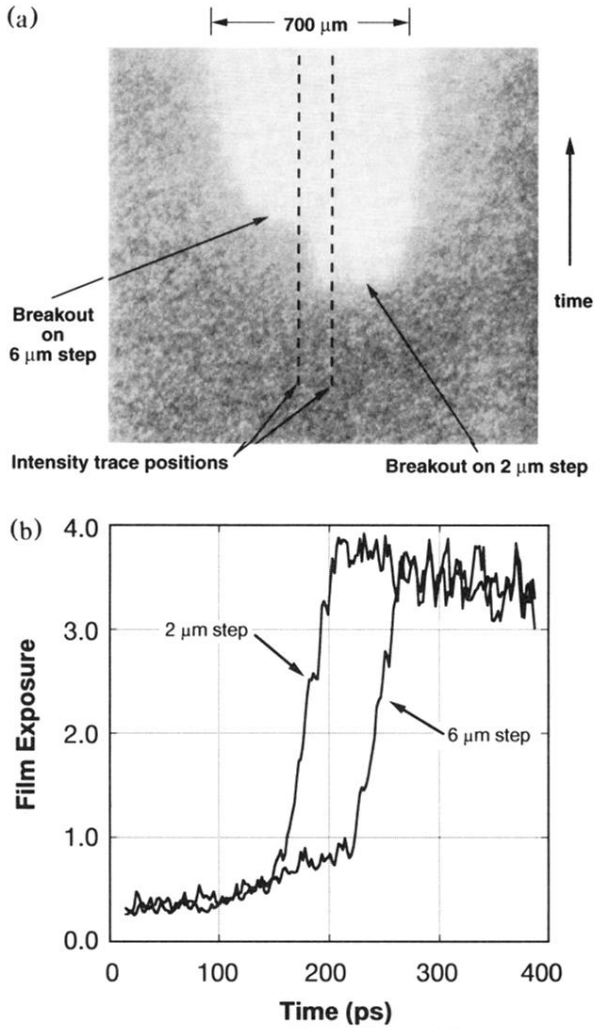

FIG. 2. Data from one experiment. (a) Streak camera record of the rear side of the target foil showing the illumination of shock breakouts on the 2 μm, earlier, and 6 μm, later, sides; (b) intensity traces vs time taken on either side of the step, along the dashed lines shown in (a). The interval between the traces provides the shock travel time across the 4 μm step difference. The interval is about 57 psec, indicating a shock speed of 70 km/sec. From the SESAME EOS tables a pressure of 0.74 Gbar is deduced from this shock speed [16].